Local Destabilization of the Tropomyosin Coiled Coil Gives the Molecular Flexibility Required for Actin Binding†

Abhishek Singh* and Sarah E. Hitchcock-DeGregori

Department of Neuroscience and Cell Biology, UMDNJ-Robert Wood Johnson Medical School, 675 Hoes Lane, Piscataway, New Jersey 08854

Received May 20, 2003; Revised Manuscript Received September 15, 2003

ABSTRACT: Tropomyosin, a coiled coil protein that binds along the length of actin filaments, contains 40 uninterrupted heptapeptide repeats characteristic of coiled coils. Yet, it is flexible. Regions of tropomyosin that may be important for binding to the filament and for interacting with troponin deviate from canonical coiled coil structure in subtle ways, altering the local conformation or energetics without interrupting the coiled coil. In a region rich in interface alanines (an Ala cluster), the chains pack closer than in canonical coiled coils, and are staggered, resulting in a bend [Brown et al. (2001) *Proc. Natl. Acad. Sci. U.S.A. 98*, 8496−8501]. Brown et al. suggested that bends at alanine clusters allow tropomyosin to wind on the actin filament helix. Another explanation is that local destabilization of the coiled coil, rather than close packing of the chains at Ala clusters per se, allows flexibility. Changing three Ala residues to canonical interface residues, A74L−A78V−A81L, greatly stabilized tropomyosin, measured using circular dichroism and differential scanning calorimetry, and reduced actin affinity >10-fold. Normal actin affinity and stability were restored in a mutant A74Q−A78N−A81Q that mimicked the stability of the Ala cluster but not the close packing of the chains. Analysis and modeling of comparable mutations introduced closer to the N-terminus show that the effects on stability and function depend on context. Models based on tropomyosin crystal structures give insight into possible effects of the mutations on the structure. We conclude that the significance of the Ala clusters in allowing flexibility of tropomyosin is stability-driven.

The α-helical coiled coil is a widespread structural motif, primarily viewed as a mechanism for formation of rod-shaped fibrous proteins, including myosin and tropomyosin, and for subunit association of globular proteins (*1*). Francis Crick predicted that a structure containing a 7-fold repeating pattern of hydrophobic residues is important for the knobs-into-holes packing at the interface between the two α-helices (*2*). In this pattern, the residues in the heptapeptide repeat are referred to as *a*−*b*−*c*−*d*−*e*−*f*−*g*. The *a* and *d* residues pack at the interface and are generally hydrophobic, while the *e* and *g* residues often have opposite charges and can stabilize the coiled coil through interchain electrostatic bonds. The basic features of the coiled coil predicted by Crick were confirmed first by the amino acid sequence of tropomyosin (*3*, *4*), and later by the crystal structure of the GCN4 leucine zipper (*5*).

Tropomyosin, a two chained coiled coil that binds to actin, is a prototype that contains 40 uninterrupted heptapeptide repeats. In this regard, tropomyosin is unusual since the repeats are interrupted in most long coiled coils. For example, the coiled coil region of myosin contains "skips" or "stammers" in the pattern of hydrophobic residues (*6*). In intermediate filament proteins, the coiled coil domains are linked by noncoiled coil sequence (*7*). In the context of the basic coiled coil that drives the assembly of a two-chained, rod-shaped protein, how does the structure incorporate features that allow for tropomyosin's functions? Tropomyosin binds specifically to actin, and end-to-end association of molecules results in formation of a cable that extends the length of the actin filament (*8*, *9*). Tropomyosin's role in cooperative function requires that the coiled-coil cable be flexible on the surface of the actin filament and be able to bind to other proteins, such as troponin (*10*−*12*). Tropomyosin's flexibility is illustrated by the motions of molecules within crystals (*13*, *14*) and on the actin filament (*15*). Depending on the regulatory state, tropomyosin assumes different positions on the actin filament, moving azimuthally over an arc of up to 35° (*16*). Tropomyosin has two forms of flexibility. One is global motion in the longitudinal dimension (as in a wave) that results from bends and twists of the backbone common to α-helices (*17*). The second is local flexibility that reflects dynamic fluctuation among substates (*18*), influenced by the stability of the interface packing and side-chain mobility of interface residues. It is the local flexibility or "breathing" that is the concern of the present work. Local flexibility can contribute to the global molecular motions of tropomyosin.

In tropomyosin, coiled coil stability has been related to local side-chain flexibility. Tropomyosin has multiple independent unfolding domains that have been identified using circular dichroism (CD)[1] and fluorescence (*19*, *20*). Lehrer and colleagues have correlated the ability of pyrene on an

† Supported by NIH Grant GM36326 to S.E.H.-D.

* Department of Neuroscience and Cell Biology, University of Medicine and Dentistry of New Jersey, Robert Wood Johnson Medical School, 675 Hoes Lane, Piscataway, NJ 08854. Tel: 732−235−4528. Fax: 732−235−4029. E-mail: singha2@umdnj.edu.

[1] Abbreviations: CD, circular dichroism; DSC, differential scanning calorimetry; DTT, dithiothreitol; TM, tropomyosin.

10.1021/bi0348462 CCC: $25.00
Published on Web 11/11/2003

interface cysteine to form pyrene excimers (and give the resulting pyrene excimer fluorescence) with local unfolding of the coiled coil, as measured using CD (*21*). The side-chain must be mobile to form pyrene excimers. The correlation of local side-chain flexibility with stability is corroborated by the effect of a cardiomyopathy-causing mutation in which decreased stability is associated with increased pyrene excimer fluorescence of a probe close to the mutation (*22*). Subtle changes in the sequence from preferred coiled coil residues may alter the local conformation or local energetics to allow for side-chain flexibility or bending without full interruption of the coiled coil structure. Compared to short leucine zippers that function primarily as oligomerization domains, such as that in GCN4 (*23*), the tropomyosin coiled coil is far from perfect. Tropomyosin has a relatively high frequency of Ala and other small hydrophobic residues in the *a* and *d* interface positions that have a quasi-periodic distribution (*24*−*26*). The presence of multiple unfolding domains in tropomyosin analyzed using calorimetry, CD, pressure denaturation, and fluorescence of specific probes, has led to the idea that regions of stable coiled coil are interrupted by less stable segments (*20*, *27*−*29*). The Ala clusters, where the α-helices are closer together and staggered (*26*), would allow for bends (*25*, *26*, *30*) and may also be sites of local conformational instability. McLachlan and Stewart suggested that the periodic Ala clusters are genetic in origin (*25*, *31*). The Ala clusters are conserved in higher eucaryotes, and one is found in *Saccharomyces pombe* (*32*), but they are absent from *Saccharomyces cerevisae* tropomyosin (*33*) that instead contains interruptions in the heptapeptide repeat of the coiled coil (*34*).

Our studies of tropomyosin and troponin T show that the sequences of regions involved in, or important for, binding interactions are not optimal for coiled coil stability and that mutations that increase stability can result in loss of function (*35*−*37*). We hypothesize (*38*) that regions of stable, canonical coiled coil function primarily as oligomerization motifs, whereas less stable, or noncanonical coiled coil, such as in an Ala cluster of tropomyosin (*26*) or in the parallel or splayed α-helices of the C-terminus of striated muscle tropomyosin (*38*, *39*), are regions of functional importance for local flexibility or binding to target proteins. We made mutations in tropomyosin at an Ala cluster located about one-third from the N-terminus that influence the stability and packing of the hydrophobic core. The results reported herein support the hypothesis and show that the stability of the tropomyosin coiled coil, but neither the sequence per se of the interface residues nor the proximity of the α-helices is important for actin affinity. We suggest that subtle modifications in the energetics of coiled coils are important for functional interactions of the coiled coil class of proteins.

MATERIALS AND METHODS

DNA Construction and Protein Purification. TM2 variants were made from rat α-TM2 cDNA (*40*, *41*) cloned in pET11d (*41*) at NcoI and BamH1 sites for expression into *Escherichia coli*. The TM2 cDNA includes the alternatively expressed exons 1a, 2b, 6b, and 9d, as well as the constitutively expressed exons 3, 4, 5, 7, and 8 (*42*, *43*).

The oligonucleotides coding each mutant TM2 were used to carry out a two-stage PCR (*44*) using Pfu turbo DNA polymerase (Stratagene, La Jolla, CA). Mutations of the alanines in period 1 (residues 18, 22, and 25) and in period 2 (residues 74, 78, and 81) were made with the oligonucleotides listed below and their reverse complements. In addition, the period 2 mutagenic oligonucleotides introduced a silent XhoI restriction site to facilitate screening. The mutagenic codons are underlined. All oligonucleotides were synthesized and PAGE purified by Integrated DNA Technologies (Skokie, Illinois).

A18L−A22V−A25L: 5′-CTCGACAAAGAGAACCTG-CTCGATCGAGTTGAGCAGCTGGAGGCTGACAAGA-AGG-3′

A18Q−A22N−A25Q: 5′-CTCGACAAAGAGAACCAG-CTCGATCGAAACGAGCAGCAGGAGGCTGACAAGA-AGG-3′

A74L−A78V−A81L: 5′-GGAGAAACTGGAGCTGCTC-GAGAAAAAGGTTACAGACCTGGAAGCTGACGTAG-CATCTC-3′

A74Q−A78V−A81L: 5′-GGAGAAACTGGAGCTGCAG-GAGAAAAAGGTTACAGACCTCGAAGCTGACGTAGC-ATCTC-3′

A74L−A78N−A81L: 5′-GGAGAAACTGGAGCTGCTC-GAGAAAAAGAACACAGACCTGGAAGCTGACGTAG-CATCTC-3′

A74L−A78V−A81Q: 5′-GGAGAAACTGGAGCTGCTC-GAGAAAAAGGTTACAGACCAGGAAGCTGACGTAG-CATCTC-3′

A74Q−A78N−A81Q: 5′-GGAGAAACTCGAGCTGCAG-GAGAAAAAGAACACAGACCAGGAAGCTGACGTAG-CATCTC-3′

The PCR product was treated with Dpn I to digest wild-type template DNA and transformed into *E. coli* DH5α cells. Plasmids containing the cDNA were isolated from single colonies and the complete cDNA was sequenced (UMDNJ DNA Synthesis and Sequencing Facility, Robert Wood Johnson Medical School, Piscataway, NJ).

The tropomyosins were expressed in *E. coli* BL21 (DE3) (*41*) and purified as previously described (*40*, *45*). The protein concentrations of TM stock solutions were determined from measurements of their difference in tyrosine absorbance at pH 6.0 and 12.5 in 6 M guanidine-HCl (*46*, *47*). Chicken pectoral muscle actin was purified as previously described (*48*). The F-actin concentration was determined using an extinction coefficient of $A_{280} = 1.1$ (0.1%).

Confirmation of Proteins by Mass Spectrometry. The molecular weights of the critical period 2 tropomyosin mutants were determined by electrospray mass spectrometry at the W. M. Keck Foundation Biotechnology Resource Laboratory (Yale University, New Haven, CT). The observed masses corresponded well to the calculated values. A74L−A78V−A81L, calculated 32 821, observed 32 818 ± 6; A74Q−A78N−A81Q, calculated 32 866, observed 32 862 ± 6.

Actin Binding Assays. Binding of tropomyosin to actin was measured by cosedimentation (*40*, *49*). Tropomyosin (0.12−8 μM, depending on the tropomyosin) and actin (5 μM) were cosedimented at 20 °C in 200 mM NaCl, 10 mM Tris-HCl, pH 7.5, 2 mM $MgCl_2$, and 0.5 mM dithiothreitol (DTT). Pellets and supernatants were analyzed using 12% SDS−polyacrylamide gels and stained with Coomassie Blue and quantified using a Molecular Dynamics model 300A computing densitometer (Sunnyvale, CA). Apparent binding

constants (K_{app}) and Hill coefficents (α_H) were determined by fitting the data to the Hill equation using SigmaPlot (Jandel Scientific):

$$v = (n[TM]^{\alpha H}K_{app}^{\alpha H})/(1 + [TM]^{\alpha H}K_{app}^{\alpha H}) \quad (1)$$

Circular Dichroism Measurements. Thermal stability measurements were made by following the ellipticity of TM at 222 nm as a function of temperature in 0.5 M NaCl, 10 mM sodium phosphate pH 7.5, 1 mM EDTA, and 0.5 mM DTT using an Aviv model 62 DS spectropolarimeter (*20*). Data were obtained at 0.2 °C intervals with a protein concentration of 0.1 mg/mL. The apparent T_m and the thermodynamic parameters for TM unfolding were calculated based on the assumption that the unfolding could be fit by up to three independent helix−coil transitions with dissociation accompanying the helix−coil transition at the highest temperature, as previously described (*24*).

Differential Scanning Calorimetry Measurements. Calorimetric measurements were performed on a model 6100 Nano II differential scanning calorimeter (Calorimetry Sciences Corp., American Fork, UT) with 0.3 mL cells from 0 °C to either 100 or 110 °C at a rate of 1 °C/min, pressure of 2 atm, and a 1 mg/mL protein concentration in 0.5 M NaCl, 10 mM sodium phosphate pH 7.5, 1 mM EDTA, and 0.5 mM DTT. The reversibility of the thermal transitions was checked by five heating and cooling runs. The calorimetric traces were corrected for the instrumental background by subtracting a scan with buffer in both cells. All calculations were carried out using CpCalc, a Windows based program supplied by the DSC vendor. A molecular mass of 66 kDa was used for coiled coil TM dimers.

Modeling. Modeling was carried out using SYBYL (Tripos, Inc.) on the TM81 2 Å crystal structure [(*26*), PDB entry 1IC2] or the 7 Å crystal structure of full-length tropomyosin [(*50*), PDB entry 1C1G]. The TM2 sequence from residues 67 to 88 was substituted for the corresponding residues in the Ala cluster in the structure, residues 11−32. Hydrogens and Gastiger-Hückel charges were added and the structure was minimized to convergence. MOLMOL (*51*) was used to calculate hydrogen bonding, bond distances, and solvent accessible surfaces. This procedure was repeated for each mutation that was made.

To test the validity of the modeling, bond distances and packing in the minimized crystal structure of TM81 were determined in the alanine cluster region, as well as in a canonical coiled coil region. The distances with the naturally occurring sequence were compared to those in the model where the alanine cluster sequence of period 2 replaced that in period 1. The mutations were introduced and compared to the wild-type model. Similar calculations were made using the 7 Å crystal structure. The inter- and intrachain bond distances and packing were similar supporting this as a valid approach. The degree of solvent accessibility was determined by using the CalcSurface function in MOLMOL which returns the accessible surface of each residue in the context of the molecule.

RESULTS AND DISCUSSION

Rationale and Mutant Design. To understand the relationship between stability and actin affinity of tropomyosin as it pertains to the core Ala clusters, we made a series of mutations to stabilize or destabilize the core using residues other than Ala. The first three periods of tropomyosin's seven repeats (*25*, *31*, *52*−*54*) contain highly conserved Ala clusters. Mutagenesis of period 2 offered us the best opportunity to correlate function and stability with the interface residues. Period 2 (residues 39−80) is the most primitive from an evolutionary point of view (*31*), and its sequence is similar to that of an "ancestral" 42-residue segment (*25*). Deletion of period 2 and modifications of the first half of period 2 (N-terminal to the Ala cluster) have small effects on the function of striated muscle α-tropomyosin, compared to other periods, especially period 1 (*37*, *55*−*59*). We made the mutations in rat α-TM2, a 284-residue tropomyosin expressed in nonmuscle cells. Unacetylated, recombinant TM2 binds well to actin in the absence of troponin (*60*).

We mutated three alanines in period 2, A74 (*d* position), A78 (*a*) and A81 (*d*). To create a canonical coiled coil with improved packing, and greater hydrophobicity and stability, we changed the *d* position alanines to Leu and the *a* position Ala to Val to make the triple mutant, A74L−A78V−A81L. A second set of mutations mimicked the stability of Ala, but not the hydrophobicity or packing, substituting Asn at the *a* position and Gln at the *d* position alanines, creating the mutant A74Q−A78N−A81Q. Asn and Gln in the *a* and *d* positions, respectively, have similar stability to Ala and also promote formation of two-chained coiled coils in model peptides (*61*−*63*). We also made mutants predicted to be intermediate in stability where one residue of the canonical coiled coil mutant was changed to Gln or Asn: A74Q−A78V−A81L; A74L−A78N−A81L; A74L−A78V−A81Q.

Analysis of Coiled Coil Stability in Protein Unfolding Studies. We measured the temperature dependence of unfolding at 222 nm using circular dichroism (CD) and found the qualitative effect of the mutations on coiled coil stability was that predicted from the design (Figure 1A, Table 1). The wild-type TM2 unfolds with three transitions (observed in the first derivative of the isotherms, Table 2) of which the final and major transition corresponds to the N-terminal region of TM2 (*29*) where our mutations are located. The mutations to create a canonical coiled coil, A74L−A78V−A81L, increased the stability (T_m) of the N-terminal transition by more than 40 °C, and the protein was not completely unfolded at 90 °C, consistent with creation of a nine heptad stretch of stable coiled coil. In contrast, the overall stability of A74Q−A78N−A81Q was closer to wild-type TM2, but with only two transitions (Table 2). The mutants with one canonical coiled coil residue changed to Asn or Gln, A74Q−A78V−A81L, A74L−A78N−A81L, and A74L−A78V−A81Q, exhibited intermediate stability. The major, N-terminal transitions were approximately 20 °C more stable than wild-type, but considerably less stable than the canonical coiled coil mutant. All mutants unfolded cooperatively, except A74L−A78V−A81L, which was still partially folded at 90 °C (Figure 1A).

Differential scanning calorimetry (DSC) was carried out on wild-type TM2, A74L−A78V−A81L, and A74Q−A78N−A81Q to demonstrate that thermal unfolding of the secondary structure is accompanied by absorption of heat. The T_m and ΔH values obtained from DSC were comparable to CD isotherms at 222 nm (Figure 1B, Table 2). The slightly

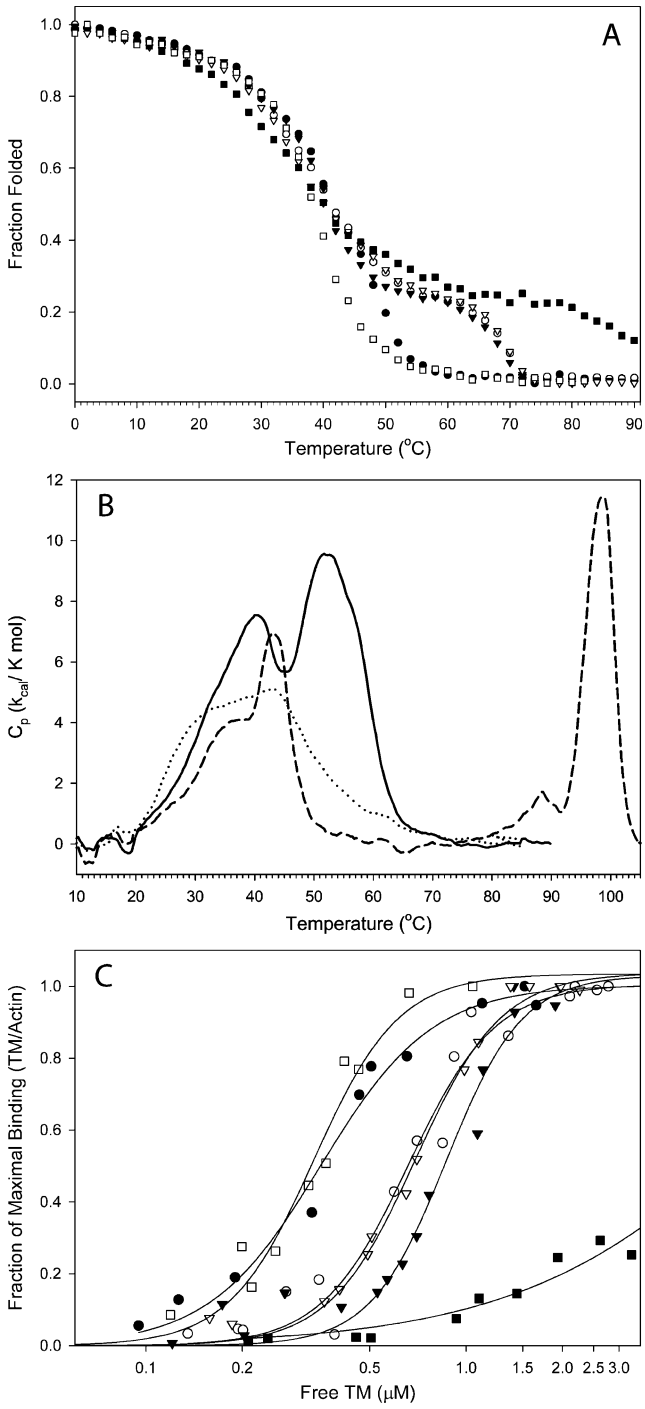

FIGURE 1: Mutations in period 2 of rat TM2. (A) Fraction folded as measured by relative ellipticity at 222 nm as a function of temperature. Wild-type TM2 (●), A74L−A78V−A81Q (○), A74L−A78N−A81L (▼), A74Q−A78V−A81L (▽), A74L−A78V−A81L (■), and A74Q−A78N−A81Q (□). Conditions: 0.1 mg/mL (1.6 μM), in 500 mM NaCl, 10 mM sodium phosphate, 1 mM EDTA, and 1 mM DTT, pH 7.5. (B) Heat capacity functions of wild-type TM2 (solid line), A74L−A78V−A81L (dashed line), and A74Q−A78N−A81Q (dotted line). Conditions: 1.0 mg/mL (15 μM) at 2 atm pressure in same buffer as Figure 1A. (C) Actin binding: wild-type TM2 (●), A74L−A78V−A81Q (○), A74L−A78N−A81L (▼), A74Q−A78V−A81L (▽), A74L−A78V−A81L (■), and A74Q−A78N−A81Q (□). Conditions: TM2 was cosedimented with actin (5 μM) at 20 °C in 200 mM NaCl, 10 mM Tris-HCl, pH 7.5, 2 mM $MgCl_2$, and 0.5 mM DTT. The data are from two or three experiments. Stoichiometric binding of 1 TM:7 actin is represented by the 1.0 fraction of maximal binding. A74L−A78V−A81L binding ratio is calculated relative to the value at saturation for wild-type.

Table 1: Actin Affinity and T_m's of the N-Terminal Unfolding Transition from the Ellipticity at 222 nm of Tropomyosin Mutants

tropomyosin	K_{app} ($\times 10^6$ M^{-1})[a]	CD T_m (°C)[b]
Period 2 Mutants		
wild-type	2.8 ± 0.2	49
A74L−A78V−A81L	~0.1	86
A74Q−A78V−A81L	1.4 ± 0.04	69
A74L−A78N−A81L	1.2 ± 0.05	68
A74L−A78V−A81Q	1.5 ± 0.1	69
A74Q−A78N−A81Q	3.0 ± 0.2	ND[c]
Period 1 Mutants		
A18L−A22V−A25L	1.5 ± 0.08	56
A18Q−A22N−A25Q	$\ll 10^5$	ND[c]

[a] The values for K_{app}, shown with standard errors. The data in Figures 1C and 3B were fit to the Hill equation, and the K_{app} is that reported by SigmaPlot for measurements at 200 mM NaCl (See Methods). The Hill coefficients were ~3 for all tropomyosins with a measurable K_{app}. At 100 mM NaCl, the K_{app} for wild-type TM2 and the A74L−A78V−A81L mutant were 5.6×10^6 and 0.51×10^6 M^{-1}, respectively. [b] The T_m is the observed midpoint of the third and final transition corresponding to the N-terminal region of TM2 (*29*). ND: no distinct final transition was observed. These two variants unfolded with a single major transition with a lower T_m than the N-terminus of wild-type TM2. All tropomyosins were fully folded and ~100% α-helical at 0 °C on the basis of mean residue ellipticity. [c] The N-terminus unfolds with the second transition, without a distinct third transition as in wild-type TM2. The overall T_m (at which the ellipticity at 222 nm, normalized to a scale of 0 [at 0 °C] to 1.0 [at 82.4 °C] was equal to 0.5) was 44.1 °C for wild-type TM2, 39.4 °C for A74Q−A78N−A81Q, and 40.9 °C for A18Q−A22N−A25Q.

higher DSC T_m and ΔH values reflect the higher protein concentration used for DSC (1 mg/mL versus 0.1 mg/mL). In comparison to the wild-type TM2, A74L−A78V−A81L and A74Q−A78N−A81Q both had lower total ΔH and ΔS values. The increase in the hydrophobic character of the core with the addition of the Leu and Val residues in A74L−A78V−A81L likely resulted in this decrease when compared to wild-type. The unfolding of all three proteins was almost completely reversible (Figure 1B). Deconvolution analysis of the wild-type TM2 indicated the presence of four distinct transitions, consistent with previously published DSC work on full-length tropomyosins (*27*, *64*). Of the four transitions, the final two correspond to the N-terminal transition observed with CD (reported in Table 2). A74L−A78V−A81L demonstrated a large shift in the final two DSC transitions, whereas the A74Q−A78N−A81Q did not have the last transition. The final transition present in the DSC of the A74L−A78V−A81L was not present in the CD studies. Due to the added pressure during the DSC runs, it was possible to scan beyond 100 °C and therefore observe the complete unfolding of the A74L−A78V−A81L mutant.

Analysis of Interface Packing using Molecular Modeling and Relationship to Stability. We carried out modeling and energy minimization analyses based on the Ala cluster in the 2.1 Å structure of the N-terminal 81 amino acids of tropomyosin (*26*). We modeled residues 67−88, containing the Ala cluster in period 2, or the mutations, into the 2.1 Å structure of the Ala cluster in period 1, replacing residues 11−32. The results give insight into the driving force behind the observed stability−sequence relationship. In the wild-type and A74L−A78V−A81L mutants, the side-chains are buried in the hydrophobic core, although the small Ala side-chains of the wild-type pack poorly, reflecting its lower stability (Figure 2A,B). The core packing of the A74Q−

Table 2: T_m, ΔS, and ΔH of Unfolding from the Ellipticity at 222 nm and DSC of Tropomyosin Mutants

	transition 1		transition 2		transition 3		transition 4		total ΔH_{cal}	
	T_m	ΔH	T_m	ΔH	T_m	ΔH	T_m	ΔH	ΔH	ΔS k_{cal}/(K mol)[a]
DSC[a]										
wild-type	32.5	46	39.8	65	52.0	62	54.2	66	239	0.7
A74L−A78V−A81L	32.3	40	42.5	65	88.3	14	98.2	70	189	0.5
A74Q−A78N−A81Q	30.9	52	42.4	54	51.5	34	ND	ND	140	0.5
CD[b,c]										
wild-type	31.4	15	39.6	40	48.4	163	ND	ND	218	
A74L−A78V−A81L	35		38.4		86.0		ND	ND		
A74Q−A78N−A81Q	27.6	13	39.1	123	ND	ND	ND	ND	136	

[a] T_m, ΔH, and ΔS values were obtained by doing a two-state fit to the excess heat capacity function in CpCalc. Deconvolution analysis resulted in four transition temperatures, or T_m values. The final two T_m transitions correspond to the N-terminal transition temperatures from CD. A74L−A78V−A81L was completely unfolded at 105 °C. A T_m of 98 °C was not observed in the CD melt. The T_m at 88 °C corresponds to the CD melt T_m of 86 °C indicating that this mutant was not completely unfolded in the CD experiments. [b] For CD, the T_m is the observed midpoint of the third and final transition corresponding to the N-terminal region of TM2. ND: no distinct transition was observed. All tropomyosins were fully folded and ~100% α-helical at 0 °C on the basis of mean residue ellipticity. [c] Estimate of the total ΔH of unfolding as obtained by curve fitting of period 2 melts to three independent helix-coil transitions with dissociation accompanying the helix-coil transition at the highest temperature in SigmaPlot. Total ΔH values are similar to DSC, however, the values corresponding to individual transitions differ. No ΔH values could be extracted for A74L−A78V−A81L because it was not completely unfolded at 95 °C.

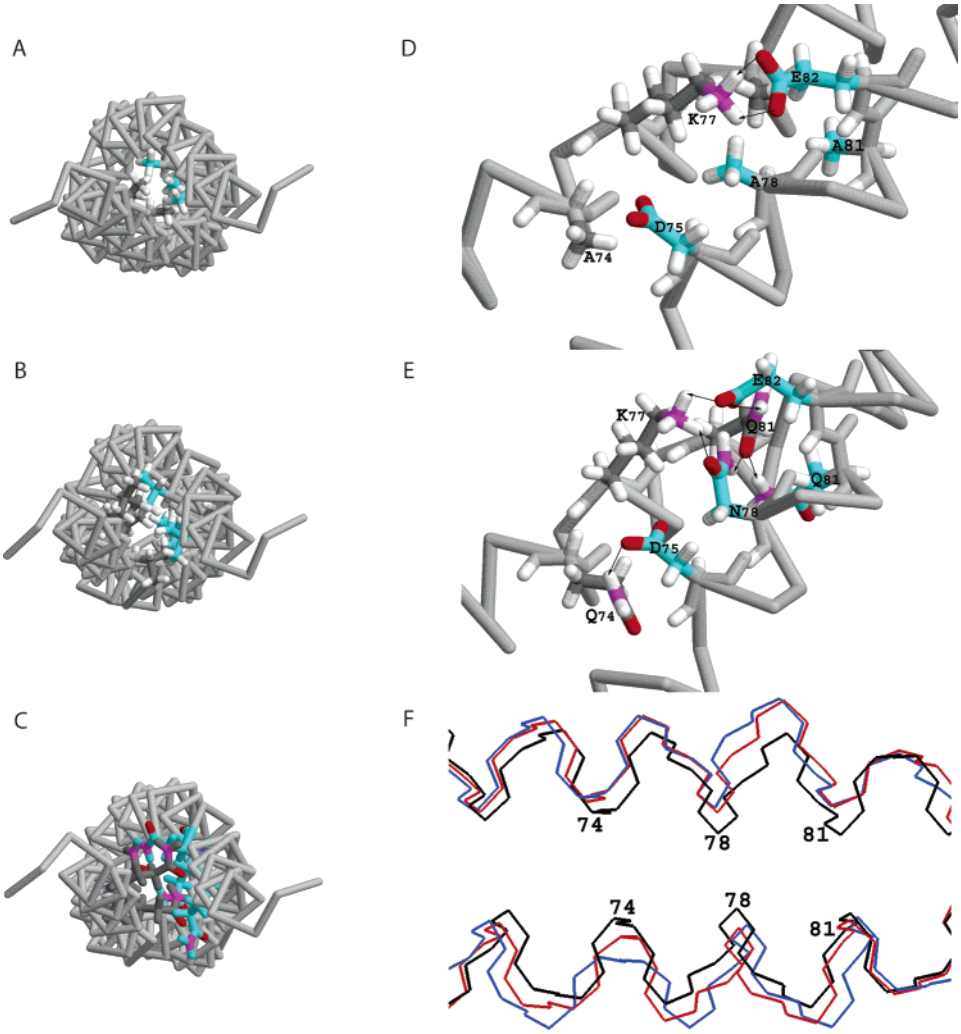

FIGURE 2: Modeling of TM2 period 2 mutations. (A−C) Views of the modeled TM2 packing through the core axis: (A) wild-type TM2; (B) A74L−A78V−A81L; and (C) A74Q−A78N−A81Q. Each view depicts the side-chains of residues 74, 78, and 81 of both chains (dark gray and aqua) with hydrogens in white, oxygens in red, and nitrogens in magenta. Side views illustrate the differences between the side-chain interactions in this region between wild-type TM2 (D) and A74Q−A78N−A81Q (E). Arrows indicate possible hydrogen and electrostatic interactions. Superposition of three of the backbones (F): wild-type (black), A74L−A78V−A81L (blue), and A74Q−A78N−A81Q (red) illustrates the shift in the backbone as a result of the mutations.

A78N−A81Q mutant was also poor. The Asn and Gln side-chains bend away from the interface to allow exposure of the hydrophilic amide groups, leaving only the α carbons of Asn and the α and β carbons of Gln buried (Figure 2C). In this regard, the A74Q−A78N−A81Q interface is similar to that of wild-type.

The wild-type coiled coil is stabilized through the interactions of Ala residues 74, 78, and 81 with neighboring *a* and *d* position residues. The *e* (Asp75 and Glu82) and *g* (Lys77) position residues form interchain electrostatic bonds (Figure 2D). These canonical interactions were preserved in the A74L−A78V−A81L mutant.

In the A74Q−A78N−A81Q mutant, however, exposure of the hydrophilic amide groups of Gln74, Asn78, and Gln81 leads to rearrangement of the ionic and polar interactions. The distortion of the Asn residues allows for formation of new intermolecular hydrogen bonds in A74Q−A78N−A81Q, detailed in Figure 2E, and results in a more stable interface than anticipated for large polar side-chains. The exposed amides maximize stability by each forming hydrogen bonds that disrupt the canonical interchain *e*−*g* interactions: Gln 74 (*d*) to Asp 75 (*e*), Asn78 (*a*) to Lys 77 (*g*) and Gln 81 (*d*), as well as Gln81 (*d*) to Asn78 (*a*) and Gln81 (*d*). In addition, the Asn and Gln residues are stabilized by more favorable polar interactions with the solvent compared to either wild-type or A74L−A78V−A81L. An Asn with comparable interactions was seen in a tropomyosin−GCN4 leucine zipper chimera (*65*). Some of these interactions are consistent with other modeling studies (*5*, *61*−*63*, *66*). Unlike the GCN4 and Jun leucine zippers (*5*, *67*, *68*), the Asn residues do not appear to hydrogen bond with each other.

Actin Affinity. The actin affinity of the TM2 variants was measured by cosedimentation. With increased stability there was a corresponding decrease in actin affinity (Figure 1C, Table 1). The stable, canonical coiled coil mutation, A74L−A78V−A81L, reduced actin binding below a level that could be measured at 200 mM NaCl (Figure 1C), and at 100 mM NaCl the affinity was ∼10-fold weaker than wild-type. The A74Q−A78N−A81Q mutant, with similar stability to wild-type TM2, bound with wild-type TM2 affinity. In comparison, the A74Q−A78V−A81L, A74L−A78N−A81L, and A74L−A78V−A81Q mutants exhibited a ∼2-fold decrease in actin affinity, consistent with their intermediate stabilities.

The correlation between the T_m of the major unfolding transition and actin affinity is consistent with other studies where we have placed a GCN4 leucine zipper sequence at four different positions in striated muscle α-tropomyosin (*37*, *58*, *69*). When the leucine zipper sequence replaced the canonical coiled coil sequence, the stability of part of the molecule increased, but the overall effect was not great, and the tropomyosins retained reasonable actin affinity. In contrast, replacement of an Ala cluster in period 5 with a stable leucine zipper resulted in a major transition with a T_m > 20 °C higher than wild-type coincident with loss of measurable actin affinity (*37*). Introduction of the L−V−L and Q−N−Q mutations (at postions *d*−*a*−*d*) into the period 5 Ala cluster had similar effects to those in period 2 reported herein (unpublished results). Together the results support the suggestion that local instability, or flexibility, at noncanonical regions of the tropomyosin coiled coil is required for tropomyosin to bind to actin (*25*, *26*, *30*, *37*).

Mutation of the Alanine Cluster in Period 1. Since the structure of the Ala cluster near the N terminus in period 1 is known (*26*), we introduced the mutations to create a canonical coiled coil (A18L−A22V−A25L) and to alter the packing but not the stability (A18Q−A22N−A25Q). The canonical coiled coil mutant exhibited an increase in T_m of the major unfolding transition, but the increase was only

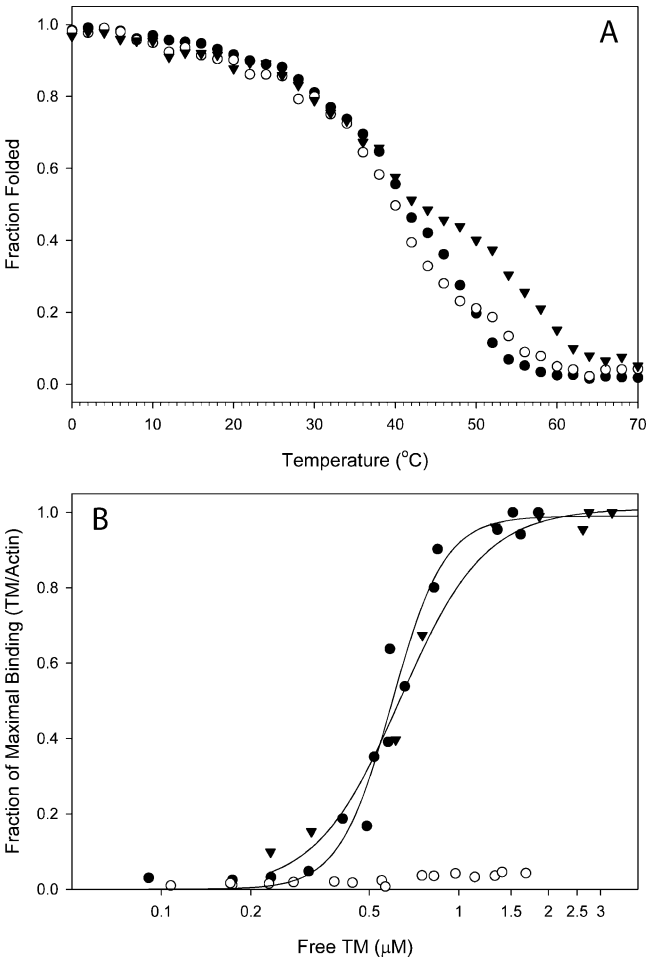

FIGURE 3: Mutations in period 1 of rat TM2. (A) Fraction folded as measured by relative ellipticity at 222 nm as a function of temperature. Wild-type TM2 (●), A18Q−A22N−A25Q (○), and A18L−A22V−A25L (▼). Conditions: same as Figure 1A. (B) Binding of period 1 mutants to actin. Wild-type TM2 (●), A18Q−A22N−A25Q (○), and A18L−A22V−A25L (▼). Conditions: same as Figure 1C.

7 °C (Figure 3A, Table 1), much less than when the mutations were introduced into the period 2 Ala cluster. Given this, it is not surprising that the actin affinity of A18L−A22V−A25L was close to wild-type (Figure 3B). In contrast, A18Q−A22N−A25Q bound poorly to actin and unfolded at a lower temperature than wild-type (Table 1).

Models of the mutants give insight into the observed differences in stability between the period 1 and 2 mutations. The noninterface residues in period 1 differ from those in period 2 and the "ancestral" period sequence (*25*). The A18Q−A22N−A25Q mutant exhibits two fewer possible hydrogen bonds than the A74Q−A78N−A81Q mutant; in period 1 Leu19 is at the *e* position corresponding to Glu75. In modeling studies, mutation of Leu19 to Glu gave similar side-chain interactions to those in period 2. We mutated the *d*−*a*−*d* Ala cluster in period 1 analogous to the region we mutated in period 2. Mutation of A22−A25−A32, an *a*−*d*−*a* cluster, where the Asn and Gln residues have comparable hydrogen bonding opportunities to those in period 2, might retain both stability and function. The impact of the mutations in period 1 on stability may also be influenced by the proximity to the N-terminus. It is well established that changes to the highly conserved N-terminus

Table 3: Effect of Changes in Core Residues on Cα Interchain Backbone Bond Distances Calculated Using MOLMOL

	TM81 Period 2 into Period 1 Distance in Å[a]		
	(wt) A74−A78−A81	A74L−A78V−A81L	A74Q−A78N−A81Q
74−74′	5.5	7.6	6.8
78−78′	4.2	5.6	5.4
81−81′	5.7	7.6	7.5
	TM81 wt Distance in Å[a]		
	(wt) A18−A22−A25	A18L−A22V−A25L	A18Q−A22N−A25Q
18−18′	5.5	7.4	7.1
22−22′	4.0	5.6	4.1
25−25′	5.7	8.2	6.8
	Full TM Period 2 Distance in Å[b]		
	(wt) A74−A78−A81	A74L−A78V−A81L	A74Q−A78N−A81Q
74−74′	5.5	8.0	7.3
78−78′	5.1	6.1	6.3
81−81′	6.8	8.7	8.0
	Full TM Period 1 Distance in Å[b]		
	(wt) A18−A22−A25	A18L−A22V−A25L	A18Q−A22N−A25Q
18−18′	5.3	7.4	6.3
22−22′	3.9	6.3	5.2
25−25′	5.8	7.8	8.0

[a] The distances were calculated in models made using the TM81 structure (*26*). For the period 2 mutants, residues 67−88 were substituted for residues 11−32 in TM81 (see Materials and Methods). [b] The distances were calculated in models made using the 7 Å structure of full-length skeletal tropomyosin (*50*).

that destabilize the coiled coil in that region result in loss of actin affinity (*49*, *57*, *70*).

Effect of the Mutations on the Modeled Interchain Distance in the Coiled Coil. In the crystal structure, the helical axis in the region of the Ala cluster is ∼2 Å closer than in regions of canonical coiled coil, and the residues are staggered, leading to a bend (*26*). In the models, based on the 2.1 Å structure (see above), the Cα interchain distances in the transposed "wild-type" Ala cluster were similar to those found in the crystal structure: ∼5.5 Å for *d* positions alanines, and ∼4 Å for the *a* position Ala (Figure 2F, Table 3), ∼1.5−2 Å closer than the interface residues in canonical coiled coil regions of the structure. In contrast, in A74L−A78V−A81L, the interchain distance increased by the expected 1.5−2 Å. In A74Q−A78N−A81Q, the interchain distances were similar to those of the canonical coiled coil. Modeling of the period 1 mutations in TM81 and of the mutations in both periods in the full-length, 7 Å structure of tropomyosin (*50*) gave similar results (Table 3).

Correlation of Modeled Structures with Experimental Analyses and Implications for Tropomyosin Function. The wrapping of tropomyosin around the actin filament helix requires two types of coiled coil deformation: local bending and sliding of the chains relative to each other (*25*, *30*). Brown et al. (*26*) postulated that the bends resulting from the staggering of the helices at the periodic Ala clusters allow for tropomyosin flexibility on the actin filament. If lower stability of the N-terminal unfolding transition reflects greater local flexibility, then interface residues other than Ala can allow the requisite flexibility for actin binding. Our modeling shows that in A74Q−A78N−A81Q the Asn and Gln exhibit less compact, Ala-type packing of the core, increasing local side-chain fluctuations. In contrast, the tighter packing of the Leu and Val of the A74L−A78V−A81L mutant would increase stability and, by being more locally rigid, may limit the ability of tropomyosin to wind around the actin helix.

The closer interchain distance at the wild-type Ala cluster appears to be less important than the packing since the effect of the interface residue mutations on stability and actin affinity does not correlate with changes in the interchain distance in the coiled coil. Our results are consistent with the recent X-ray structure of a myosin rod fragment that contains a coiled coil where the interface residues are poorly packed but the interchain distance is typical of a canonical coiled coil (*71*). We cannot address the importance of a stagger or bending since the modeled structures retained the stagger. Comparison of the effects of comparable mutations in periods 1 and 2 shows that the context of the interface mutations also influences both stability and function.

If optimal flexibility and stability are more important than the identity of the interface amino acids per se, how are the Ala clusters present in the "ancestral" 42-residue tropomyosin period (*25*) conserved through gene duplications and evolution? Alanine has high helical propensity (*72*) and is the most abundant amino acid in α-helices, along with leucine (*73*). Ala also has a high frequency in coiled coils, second to leucine in the interface positions, although the frequency in tropomyosin is unusually high (*24*, *74*). Therefore, we can presume Ala was prominent in the "ancestral" coiled coils which were modified to allow binding to actin, becoming tropomyosin. An interface alanine allows coiled coil formation, and since the side-chain is buried it does not interfere with the interactions of other side-chains with each other or target proteins. Point mutations in Ala codons would result in amino acids, with the exception of Val, that are unfavorable in the core, although apparently tolerated and retained in some cases. Asn and Gln, which are found in the *a* and *d* positions of coiled coils (although Asn is never in an *a* position in tropomyosin), would require a minimum of two base changes and probably result from point mutations of codons for other amino acids favorable for coiled coils. However, unlike Ala, the ability of Asn and Gln to form a "stable-but-not-too-stable" coiled coil depends on the identity of neighboring interface and noninterface residues.

Conclusions. The interface residues of the tropomyosin coiled coil were mutated to change the stability and packing. Analysis of the mutant proteins showed that the local flexibility, as reflected in the stability, of the coiled coil of a region of tropomyosin about one-third from the N-terminus, is important for actin binding. Modeling shows how the core residue mutations can influence the local structure and stability. We conclude that interruption of the canonical coiled coil with regions of lower coiled coil stability, and potential for increased dynamic core side-chain fluctuation, is important for tropomyosin function. The results lend support to our hypothesis that noncanonical packing of the coiled coil and resultant flexibility are important for the binding interactions and function of coiled coil proteins (*38*).

ACKNOWLEDGMENT

We are grateful to Dr. Norma Greenfield, Dr. Thomas Palm, and Dr. Barbara Brodsky for numerous discussions and for reading the manuscript. We are also grateful to Sarah Graboski for providing protein, Anton Persikov for help with DSC, and to Wamiq Chowdary for some of the early work on the TM2 A74L−A78V−A81L mutant.

REFERENCES

1. Burkhard, P., Stetefeld, J., and Strelkov, S. V. (2001) *Trends Cell Biol. 11*, 82−8.
2. Crick, F. H. C. (1953) *Acta Crystallogr. 6*, 689−97.
3. Sodek, J., Hodges, R. S., Smillie, L. B., and Jurasek, L. (1972) *Proc. Natl. Acad. Sci. U.S.A. 69*, 3800−4.
4. Stone, D., and Smillie, L. B. (1978) *J. Biol. Chem. 253*, 1137−48.
5. O'Shea, E. K., Klemm, J. D., Kim, P. S., and Alber, T. (1991) *Science 254*, 539−44.
6. Brown, J. H., Cohen, C., and Parry, D. A. (1996) *Proteins 26*, 134−45.
7. North, A. C., Steinert, P. M., and Parry, D. A. (1994) *Proteins 20*, 174−84.
8. O'Brien, E. J., Bennett, P. M., and Hanson, J. (1971) *Philos. Trans. R. Soc. London B 261*, 201−208.
9. McLachlan, A. D., and Stewart, M. (1975) *J. Mol. Biol. 98*, 293−304.
10. Perry, S. V. (1998) *J. Muscle Res. Cell Motil. 19*, 575−602.
11. Gordon, A. M., Homsher, E., and Regnier, M. (2000) *Physiol. Rev. 80*, 853−924.
12. Tobacman, L. S. (1996) *Annu. Rev. Physiol. 58*, 447−81.
13. Phillips, G. N., Jr., Fillers, J. P., and Cohen, C. (1980) *Biophys. J. 32*, 485−502.
14. Phillips, G. N., Jr., and Chacko, S. (1996) *Biopolymers 38*, 89−95.
15. Narita, A., Yasunaga, T., Ishikawa, T., Mayanagi, K., and Wakabayashi, T. (2001) *J. Mol. Biol. 308*, 241−61.
16. Vibert, P., Craig, R., and Lehman, W. (1997) *J. Mol. Biol. 266*, 8−14.
17. Emberly, E. G., Mukhopadhyay, R., Wingreen, N. S., and Tang, C. (2003) *J. Mol. Biol. 327*, 229−37.
18. Frauenfelder, H. (2002) *Proc. Natl. Acad. Sci. U.S.A. 99 Suppl 1*, 2479−80.
19. Ishii, Y. (1994) *Eur. J. Biochem. 221*, 705−12.
20. Ishii, Y., Hitchcock-DeGregori, S., Mabuchi, K., and Lehrer, S. S. (1992) *Protein Sci. 1*, 1319−25.
21. Graceffa, P., and Lehrer, S. S. (1980) *J. Biol. Chem. 255*, 11296−300.
22. Golitsina, N., An, Y., Greenfield, N. J., Thierfelder, L., Iizuka, K., Seidman, J. G., Seidman, C. E., Lehrer, S. S., and Hitchcock-DeGregori, S. E. (1997) *Biochemistry 36*, 4637−42.
23. Landschulz, W. H., Johnson, P. F., and McKnight, S. L. (1988) *Science 240*, 1759−64.
24. Conway, J. F., and Parry, D. A. (1990) *Int. J. Biol. Macromol. 12*, 328−34.
25. McLachlan, A. D., and Stewart, M. (1976) *J. Mol. Biol. 103*, 271−98.
26. Brown, J. H., Kim, K. H., Jun, G., Greenfield, N. J., Dominguez, R., Volkmann, N., Hitchcock-DeGregori, S. E., and Cohen, C. (2001) *Proc. Natl. Acad. Sci. U.S.A. 98*, 8496−501.
27. Potekhin, S. A., and Privalov, P. L. (1982) *J. Mol. Biol. 159*, 519−35.
28. Sturtevant, J. M., Holtzer, M. E., and Holtzer, A. (1991) *Biopolymers 31*, 489−95.
29. Greenfield, N. J., and Hitchcock-DeGregori, S. E. (1995) *Biochemistry 34*, 16797−805.
30. Stewart, M. (2001) *Proc. Natl. Acad. Sci. U.S.A. 98*, 8165−6.
31. McLachlan, A. D., Stewart, M., and Smillie, L. B. (1975) *J. Mol. Biol. 98*, 281−91.
32. Balasubramanian, M. K., Helfman, D. M., and Hemmingsen, S. M. (1992) *Nature 360*, 84−7.
33. Drees, B., Brown, C., Barrell, B. G., and Bretscher, A. (1995) *J. Cell Biol. 128*, 383−92.
34. Strand, J., Nili, M., Homsher, E., and Tobacman, L. S. (2001) *J. Biol. Chem. 276*, 34832−9.
35. Greenfield, N. J., Palm, T., and Hitchcock-DeGregori, S. E. (2002) *Biophys. J. 83*, 2754−66.
36. Palm, T., Graboski, S., Hitchcock-DeGregori, S. E., and Greenfield, N. J. (2001) *Biophys. J. 81*, 2827−37.
37. Hitchcock-DeGregori, S. E., Song, Y., and Greenfield, N. J. (2002) *Biochemistry 41*, 15036−44.
38. Greenfield, N. J., Swapna, G. V., Huang, Y., Palm, T., Graboski, S., Montelione, G. T., and Hitchcock-DeGregori, S. E. (2003) *Biochemistry 42*, 614−9.
39. Li, Y., Mui, S., Brown, J. H., Strand, J., Reshetnikova, L., Tobacman, L. S., and Cohen, C. (2002) *Proc. Natl. Acad. Sci. U.S.A. 99*, 7378−83.
40. Hammell, R. L., and Hitchcock-DeGregori, S. E. (1996) *J. Biol. Chem. 271*, 4236−42.
41. Studier, F. W., Rosenberg, A. H., Dunn, J. J., and Dubendorff, J. W. (1990) *Methods Enzymol. 185*, 60−89.
42. Lin, J. J., Warren, K. S., Wamboldt, D. D., Wang, T., and Lin, J. L. (1997) *Int. Rev. Cytol. 170*, 1−38.
43. Helfman, D. M., Cheley, S., Kuismanen, E., Finn, L. A., and Yamawaki-Kataoka, Y. (1986) *Mol. Cell Biol. 6*, 3582−95.
44. Wang, W., and Malcolm, B. A. (1999) *Biotechniques 26*, 680−2.
45. Hitchcock-DeGregori, S. E., and Heald, R. W. (1987) *J. Biol. Chem. 262*, 9730−5.
46. Edelhoch, H. (1967) *Biochemistry 6*, 1948−54.
47. Lehrer, S. S. (1975) *Proc. Natl. Acad. Sci. U.S.A. 72*, 3377−81.
48. Hitchcock-DeGregori, S. E., Mandala, S., and Sachs, G. A. (1982) *J. Biol. Chem. 257*, 12573−12580.
49. Heald, R. W., and Hitchcock-DeGregori, S. E. (1988) *J. Biol. Chem. 263*, 5254−9.
50. Whitby, F. G., and Phillips, G. N., Jr. (2000) *Proteins 38*, 49−59.
51. Koradi, R., Billeter, M., and Wuthrich, K. (1996) *J. Mol. Graph. 14*, 51−5, 29−32.
52. Parry, D. A. (1975) *Nature 256*, 346−7.
53. Parry, D. A. (1975) *J. Mol. Biol. 98*, 519−35.
54. Phillips, G. N., Jr. (1986) *J. Mol. Biol. 192*, 128−31.
55. Hitchcock-DeGregori, S. E., and Varnell, T. A. (1990) *J. Mol. Biol. 214*, 885−96.
56. Moraczewska, J., and Hitchcock-DeGregori, S. E. (2000) *Biochemistry 39*, 6891−7.
57. Greenfield, N. J., Stafford, W. F., and Hitchcock-DeGregori, S. E. (1994) *Protein Sci. 3*, 402−10.
58. Hitchcock-DeGregori, S. E., and An, Y. (1996) *J. Biol. Chem. 271*, 3600−3.
59. Palm, T., Greenfield, N. J., and Hitchcock-DeGregori, S. E. (2003) *Biophys. J. 84*, 3181−9.
60. Cho, Y. J., and Hitchcock-DeGregori, S. E. (1991) *Proc. Natl. Acad. Sci. U.S.A. 88*, 10153−7.
61. Tripet, B., Wagschal, K., Lavigne, P., Mant, C. T., and Hodges, R. S. (2000) *J. Mol. Biol. 300*, 377−402.
62. Wagschal, K., Tripet, B., and Hodges, R. S. (1999) *J. Mol. Biol. 285*, 785−803.
63. Wagschal, K., Tripet, B., Lavigne, P., Mant, C., and Hodges, R. S. (1999) *Protein Sci. 8*, 2312−29.
64. O'Brien, R., Sturtevant, J. M., Wrabl, J., Holtzer, M. E., and Holtzer, A. (1996) *Biophys. J. 70*, 2403−7.
65. Greenfield, N. J., Montelione, G. T., Farid, R. S., and Hitchcock-DeGregori, S. E. (1998) *Biochemistry 37*, 7834−43.
66. Lumb, K. J., and Kim, P. S. (1995) *Biochemistry 34*, 8642−8.
67. Glover, J. N., and Harrison, S. C. (1995) *Nature 373*, 257−61.
68. Junius, F. K., Mackay, J. P., Bubb, W. A., Jensen, S. A., Weiss, A. S., and King, G. F. (1995) *Biochemistry 34*, 6164−74.
69. Hammell, R. L., and Hitchcock-DeGregori, S. E. (1997) *J. Biol. Chem. 272*, 22409−16.
70. Moraczewska, J., Greenfield, N. J., Liu, Y., and Hitchcock-DeGregori, S. E. (2000) *Biophys. J. 79*, 3217−25.
71. Li, Y., Brown, J. H., Reshetnikova, L., Blazsek, A., Farkas, L., Nyitray, L., and Cohen, C. (2003) *Nature 424*, 341−5.
72. Chou, P. Y., and Fasman, G. D. (1974) *Biochemistry 13*, 222−45.
73. Negrete, J. A., Vinuales, Y., and Palau, J. (1998) *Protein Sci. 7*, 1368−79.
74. Cohen, C., and Parry, D. A. (1990) *Proteins 7*, 1−15.

BI0348462